Structure, Vol. 10, 715–724, May, 2002, ©2002 Elsevier Science Ltd. All rights reserved. PII S0969-2126(02)00764-5

Crystal Structure of the Complex between Calyculin A and the Catalytic Subunit of Protein Phosphatase 1

Akiko Kita,[1] Shigeki Matsunaga,[2] Akira Takai,[3,7] Hirotaka Kataiwa,[1] Toshiyuki Wakimoto,[2] Nobuhiro Fusetani,[2] Minoru Isobe,[4] and Kunio Miki[1,5,6]

[1]Department of Chemistry
Graduate School of Science
Kyoto University
Sakyo-ku, Kyoto 606-8502
Japan

[2]Laboratory of Aquatic Natural Products Chemistry
Graduate School of Agricultural and Life Sciences
The University of Tokyo
Bunkyo-ku, Tokyo 113-8657
Japan

[3]Laboratory of Biomolecular Dynamics
Graduate School of Medicine
Nagoya University
65 Tsurumai-cho
Showa-ku, Nagoya 466-8550
Japan

[4]The Laboratory of Bioorganic Chemistry
Graduate School of Bioagricultural Science
Nagoya University
Furo-cho, Nagoya 464-8601
Japan

[5]RIKEN Harima Institute/SPring-8
Koto 1-1-1
Mikazukicho
Sayo-gun, Hyogo 679-5148
Japan

Summary

The crystal structure of the catalytic subunit of the protein phosphatase 1 (PP1), PP1γ, in complex with a marine toxin, calyculin A, was determined at 2.0 Å resolution. The metal binding site contains the phosphate group of calyculin A and forms a tight network via the hydrophilic interactions between PP1 and calyculin A. Calyculin A is located in two of the three grooves, namely, in the hydrophobic groove and the acidic groove on the molecular surface. This is the first observation to note that the inhibitor adopts not a pseudocyclic conformation but an extended conformation in order to form a complex with the protein. The amino acid terminus of calyculin A contributes, in a limited manner, to the binding to PP1γ, which is consistent with findings from the studies of dose-inhibition analysis.

Introduction

Protein phosphatases 1 and 2A (PP1 and PP2A) are two of the four major enzymes that dephosphorylate serine and threonine residues of proteins in the cytosol of eukaryotic cells [1, 2]. These enzymes play critical roles in determining the level of phosphorylation and, hence, the biological activities of many proteins. There are several naturally occurring toxins that are now widely used because of their potent and specific actions to these structurally related enzymes, showing 50% amino acid sequence identity in the catalytic domain [1, 2]. They include okadaic acid [3], calyculin A [4], microcystin-LR (MCLR) [5], and cantharidin [6] (Figure 1).

Among these inhibitors, calyculin A, initially isolated as a potent cytotoxin from the marine sponge *Discodermia calyx*, has a unique structure, consisting of a polyketide and a dipeptide with a phosphate group in the polyketide portion [7]. A number of congeners have been reported from several sponges. Our recent study on the structure-activity relationship (SAR) using nine natural congeners and six chemical derivatives of calyculin A has identified several functional groups, such as the phosphate group, the hydroxyl at C-13, and the hydrophobic polyketide tail, as essential for the inhibitory action of the toxin on the enzymes [8]. In contrast, the dipeptide portion appears to be relatively unimportant for the interaction with the enzymes [8]. Several amino acid residues of the enzymes important for the affinity spectra of calyculin A and other inhibitors have also been identified by mutagenetic experiments [9–11].

X-ray crystallography of the catalytic subunit of PP1 (α-isozyme; PP1α) complexed with MCLR has provided a detailed view of the interaction between the enzyme and the toxin [12]. Several binding models for calyculin A, as well as those for the other inhibitors, have been proposed on the basis of this crystallographic structure [13–17]. All such models postulated that calyculin A is accommodated into the binding pocket for MCLR in such a way that the head component of calyculin A, including the aforementioned functional groups, forms hydrogen bonds or indirect coordinate bonds with the amino acid residues around the catalytic center, whereas the nonpolar polyketide tail is docked in the hydrophobic surface groove that directly extends from the catalytic center.

However, it should be noted that these models are still purely speculative. For example, no direct experimental evidence indicating the existence of specific hydrogen bonds between the enzyme and calyculin A has been available to date. Although calyculin A is known to adopt a pseudocyclic conformation by forming intramolecular salt bridges and hydrogen bonds in the solid state as well as in the solution state in aprotic solvents [15, 18], the overall conformation of calyculin A in the enzyme-bound state remains for the most part uncertain due to its flexible backbone structure. Also, the basic hypothesis of the models that calyculin A and the other phosphatase inhibitors share the same binding site with MCLR

[6]Correspondence: miki@kuchem.kyoto-u.ac.jp
[7]Present address: Asahikawa Medical College, Midorigaoka Higashi 2-1-1-1, Asahikawa 078-8510, Japan.

Key words: PP1γ-calyculin A complex; crystal structure; protein phosphatase 1 catalytic subunit (PP1c); calyculin A; PP1c-inhibitor complex

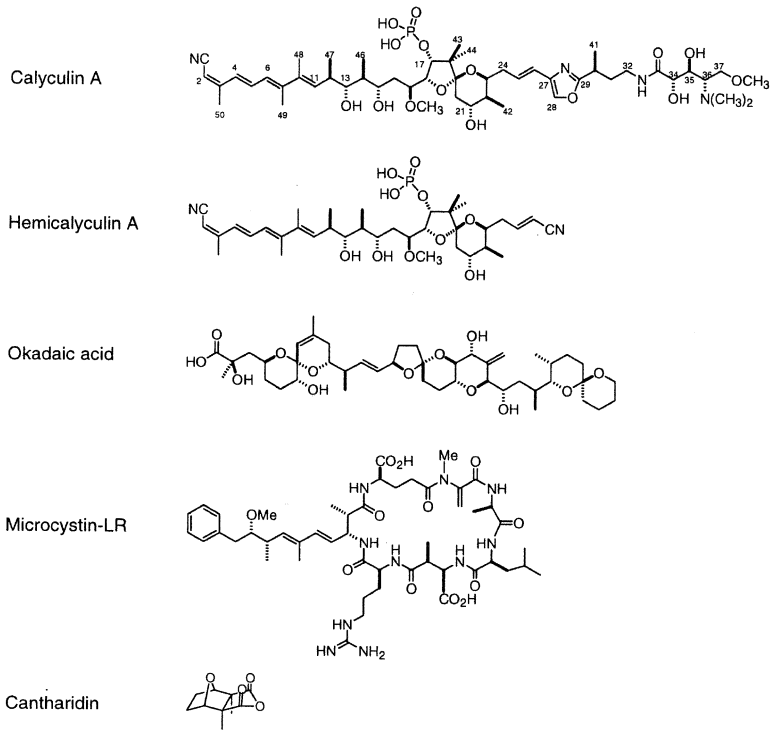

Figure 1. Structural Formulae of Calyculin A, Hemicalyculin A, Okadaic Acid, MCLR, and Cantharidin

should not be regarded as proven. This assumption is mainly based on the results of in vitro competition assays that calyculin A and the other inhibitors bind to PP1 and PP2A in a mutually exclusive manner [19]. However, the exclusiveness of interactions could alternatively be explained by assuming that the binding of an inhibitor causes a conformational change in the enzyme molecule, resulting in a decrease in its affinity to another inhibitor at a different binding site. As we pointed out previously [19], it is logically impossible to completely exclude such an alternative possibility by conventional competition assays alone.

In the present study, we have determined the three-dimensional structure of the complex between calyculin A and the γ isoform of PP1 (PP1γ) by X-ray crystallography. The structure obtained shows that calyculin A is indeed accommodated in the surface groove of PP1γ, where MCLR is also bound. Calyculin A is docked onto PP1γ with the binding mode of an extended form, which is different from the crystal structure [18] and the solution structure of calyculin A [15]. Furthermore, the bound conformation of calyculin A affords several key interactions with the enzyme.

Results and Discussion

Structure Determination

The PP1γ-calyculin A complex crystals were obtained from PEG 3350 solutions including 0.2 M potassium sulfate as an additive by the sitting drop vapor diffusion method. The working R factor for the final model, including residues 7–299 of two PP1γ molecules, 4 metal atoms assigned as Mn (see below), 2 calyculin A molecules (N1–C32), and 96 water molecules, was 0.18 for the reflections between 20.0 and 2.0 Å resolution, and the free R factor dropped to 0.22 for 5% of the total reflections. The stereochemistry of the final model was reasonable, with 88% residues lying within the most favorable regions on the Ramachandran plot. The root-mean-square (rms) deviations from the ideal values were 0.007 Å for the bond lengths and 1.43° for the angles. Superimposition of the Cα atoms of two PP1γ-calyculin A molecules in an asymmetric unit shows an rmsd of 0.21 Å. The statistics for data collection and refinement are shown in Tables 1 and 2.

Overview of the PP1γ-Calyculin A Complex

The catalytic subunit of PP1γ-calyculin A complex forms an ellipsoidal structure, which consists of 10 α helices and 14 β strands (Figure 2). On the molecular surface, there are three grooves connected at the bifurcation point (Figure 3A). The calyculin A molecule was found

Table 1. Data Collection Statistics

X-ray source	BL44-B2 (SPring-8)
Wavelength (Å)	1.00
Temperature (K)	293
Resolution limit (Å)	50–2.0
Space group	$P2_12_12$
Unit cell dimensions (Å)	98.1, 136.4, 61.6
Measured reflections	536,140
Unique reflections	56,530
Redundancy	6.2
R_{merge} (%)[a]	7.8 (39.0)[b]
Completeness (%)	99.9 (99.6)[b]

[a] $R_{merge} = \Sigma(|I - \langle I \rangle|)/\Sigma(I)$

[b] The values for the highest resolution shell (2.07–2.00 Å) are in parenthesis.

Table 2. Refinement Statistics

Resolution (Å)	20.0–2.0
R_{work} (%)/R_{free} (%)[a]	18.2/21.8
Number of atoms	
Protein	4724
Calyculin A	112
Metal	4
Solvent	96
Rms deviations from ideality	
Bond length (Å)	0.007
Bond angles (°)	1.43
Average B factors (Å^2)	
Protein	21.0
Calyculin A	18.8
Metal	14.4
Solvent	25.2
Ramachandran statistics (%)	
Most-favored regions	88.1
Additionally allowed regions	9.7

[a] $R = \Sigma||F_{obs}| - |F_{calc}||/\Sigma|F_{obs}|$.
R_{work} is calculated from a set of reflections in which 5% of the total reflections have been randomly omitted from the refinement used to calculate R_{free}.

at the grooves. The overall and secondary structures of PP1γ are similar to those of PP1α-MCLR [12], PP1γ-tungstate complex [20], and PP1γ-okadaic acid [21] complex. Strong electron densities assumed to be metal atoms were also found at the bifurcation point, where the metal atoms were found in the PP1α-MCLR structure. We assigned them as Mn atoms during the refinement due to the presence of Mn in the purification and crystallization procedures.

The groove in PP1α-MCLR is an extended Y shape that consists of a hydrophobic groove, an acidic groove, and a C-terminal groove (Figure 3B). On the other hand, the pathway to the C-terminal groove on the surface of PP1γ-calyculin A complex is closed by the Cys273

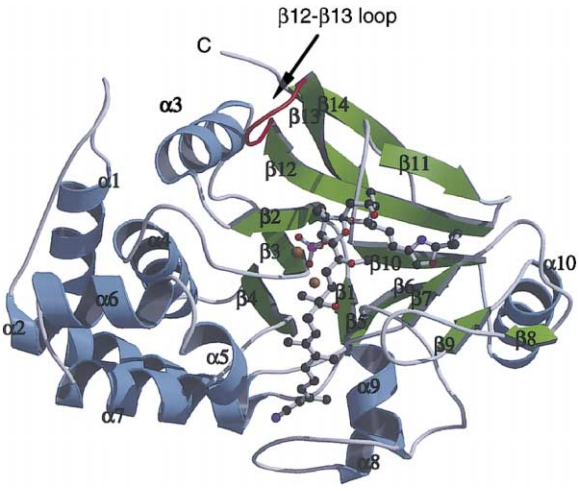

Figure 2. The Overall Structure of PP1γ-Calyculin A Complex

Schematic diagram of the three-dimensional structure of PP1γ, drawn by the program MOLSCRIPT [44], and rendered by RASTER3D [45]. The calyculin A molecule is shown in ball and stick representation. Colors are employed to identify the helices and strands. Metal ions, gold circles; β12–β13 loop, red.

A

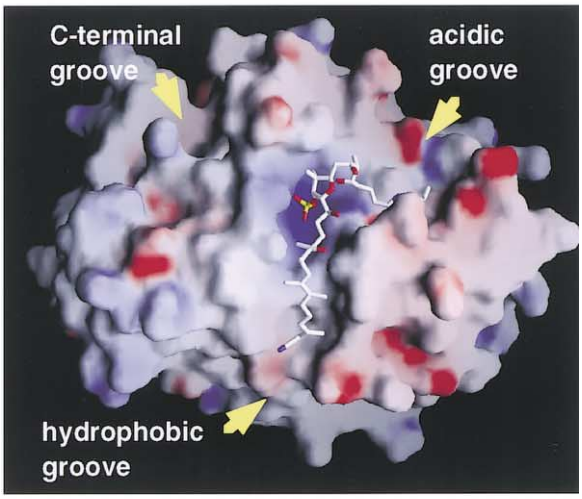

B

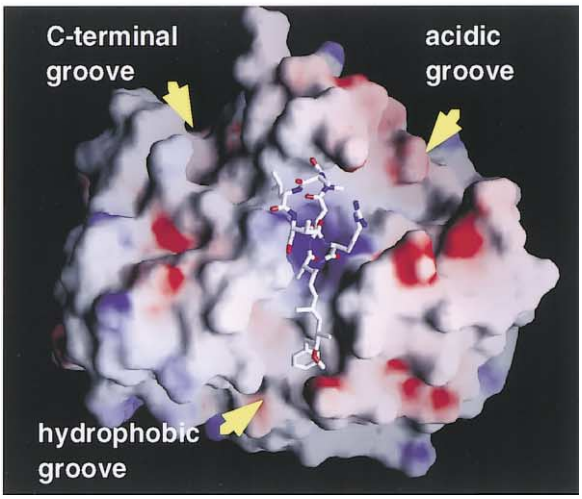

Figure 3. The Molecular Surfaces of PP1γ-Calyculin A Complex and PP1α-MCLR

They are shown in color according to their electrostatic potentials calculated by GRASP [43]: negatively charged surfaces, red; positively charged surfaces, blue. The charges of metals are assigned as +2. The orientation of the molecule is similar to that in Figure 2. The three grooves are indicated by yellow arrows.
(A) The molecular surface of PP1γ-calyculin A complex.
(B) The molecular surface of PP1α-MCLR.

belonging to the β12–β13 loop (Figure 3A). C2–C32 of calyculin A displayed very clear electron densities, whereas the electron densities of the amino acid terminus (C33–C37) of both calyculin A molecules in the asymmetric unit were not so distinct. For the association of PP1 with toxins and the inhibitors, the β12–β13 loop

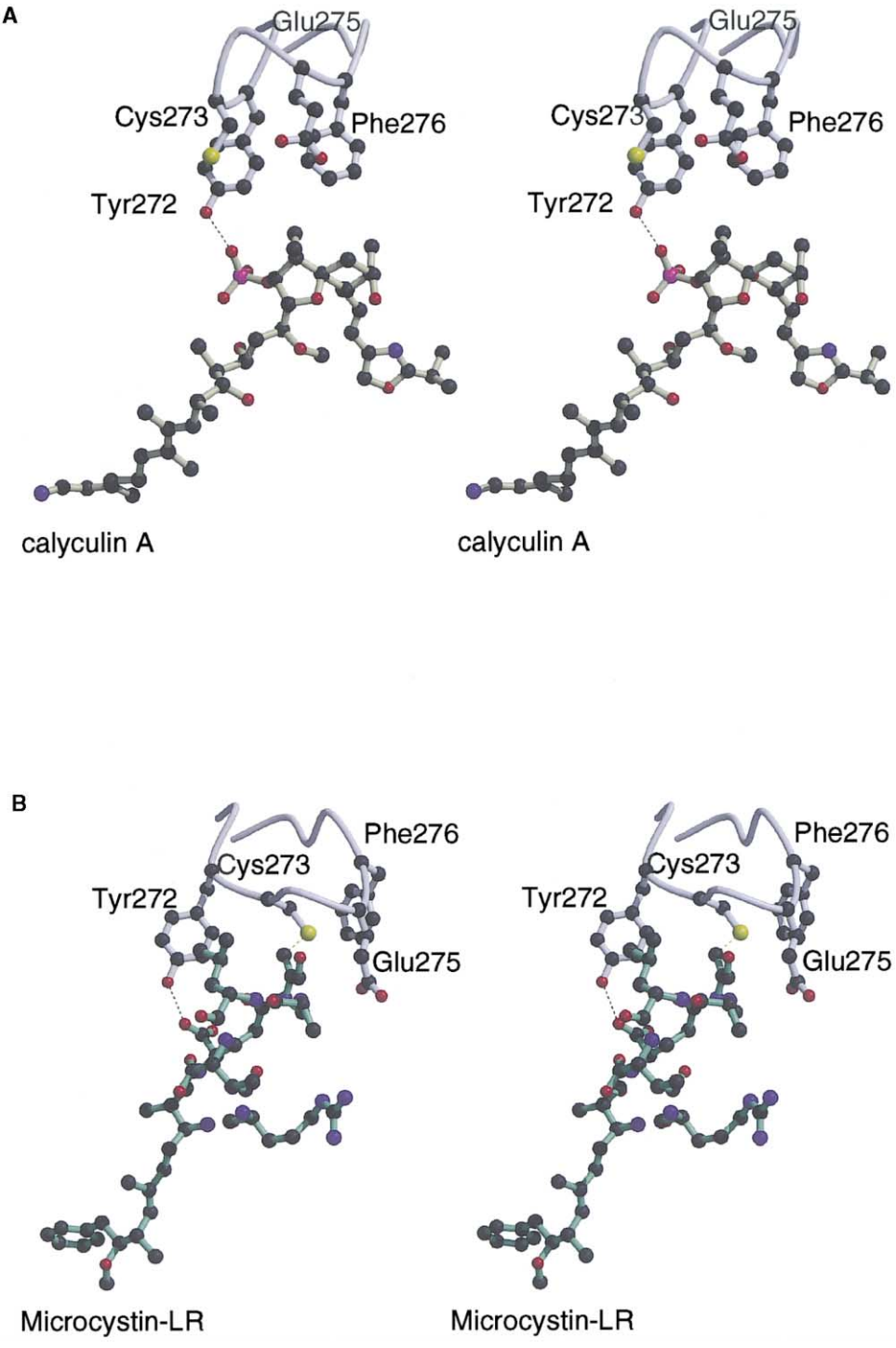

Figure 4. Stereoviews of the β12–β13 Loops and Inhibitors in PP1γ-Calyculin A Complex and in PP1α-MCLR

The residues of Tyr272, Cys273, Glu275, and Phe276 of both proteins are represented by ball and stick models. Calyculin A and MCLR are also represented by ball and stick models colored in yellow and green, respectively. The dashed black lines indicate the hydrogen bonds, and the dashed yellow line indicates the covalent bond.

(A) The β12–β13 loop in PP1γ-calyculin A complex.

(B) The β12–β13 loop in PP1α-MCLR.

is supposed to be essential [22]. The conformation of the β12–β13 loop of PP1γ-calyculin A complex is similar to that of PP1γ-okadaic acid complex [21], but not similar to that of PP1α-MCLR. The structures of the β12–β13 loops in PP1γ-calyculin A complex and PP1α-MCLR are shown together with their inhibitors in Figure 4. Only the Tyr272 residue interacted with the inhibitor in the PP1γ-calyculin A β12–β13 loop, while Tyr272 and Cys273 were

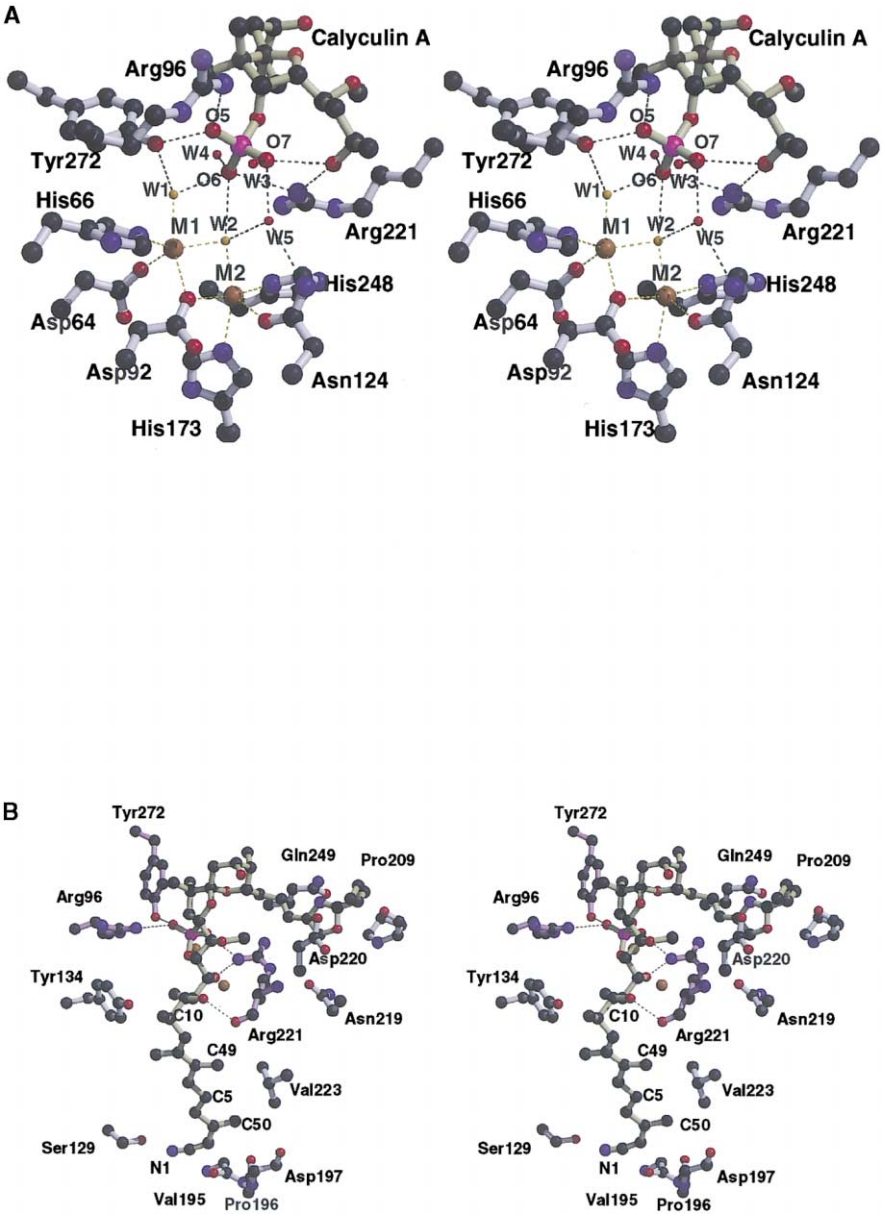

Figure 5. Calyculin A Binding Site

Calyculin A, yellow.

(A) Stereoviews of the metal and phosphate group of the calyculin A binding site. Metal ions, gold; metal-liganded water oxygen atoms, orange; other non-metal-liganded water molecules, small red circles. The dashed lines indicate the binding of two atoms, the orange dashed lines indicate metal-ligand interactions, and the black dashed lines indicate other bonds.

(B) The interactions between calyculin A and residues belonging to PP1γ. The residues within 3.5 Å from calyculin A are shown. Residues that form a hydrogen bond or salt bridge with calyculin A, purple. The black dashed lines indicate hydrogen bonds and salt bridges. The N1, C50, C5, C49, and C10 atoms of calyculin A are marked in the figure.

shown to bind with the side chain of the inhibitor in PP1α-MCLR. Cys273 in PP1α-MCLR is covalently linked to MCLR [12]. In the PP1γ-calyculin A complex, a large electron density of Sγ of Cys273 was observed. Cys273 might be oxidized with a terminal sulfinyl group in PP1γ-calyculin A complex.

Metal Binding Site

As mentioned above, we assumed the strong electron densities located at the groove bifurcation to be Mn atoms (M1 and M2). At the metal binding site, the phosphate group of calyculin A, two ligand water molecules (W1 and W2), and three nonligand water molecules (W3, W4, and W5) were observed (Figure 5A). M1 is coordinated by the four equatorial ligands provided by two protein side chains (the Nε2 atom of His 66 and the Oδ2 atom of Asp92) and two water molecules (W1 and W2). W1 is hydrogen bonded to the O6 atom of the phosphate group of calyculin A and to the hydroxyl oxygen of Tyr272. The O6 atom of the phosphate group also forms

a hydrogen bond with W2. The Oδ1 atom of Asp64 is the axial ligand of M1. The coordination geometries around both M1 and M2 are distorted square pyramids. M2 shares W2 and the Oδ2 atom of Asp92 with M1 as the bridging ligands for two metals. The four equatorial ligands of M2 are W2, the Oδ2 atom of Asp92, the Nε2 atom of His173, and the Nδ1 atom of His248. The axial ligand of M2 is the Oδ1 atom of Asn124. The average distance between M1 and M2 is 3.2 Å, which is similar to that of PP1α-MCLR.

At the active site, the metals, ligand atoms, water molecules, and the phosphate group of calyculin A form a close network (Figure 5A). W4 binds to the phosphate O6 atom and the main chain N atom of Val250. The W3 oxygen atom forms hydrogen bonds with the phosphate O7 atom and the Nε2 atom of His125, which supposedly plays a critical role in the dephosphorylation reaction. The Nε2 of His125 forms a hydrogen bond with W5, which forms hydrogen bonds with Nδ2 of Asn124, W2, and the O5 phosphate of calyculin A. The O5 phosphate atom of calyculin A binds to the guanidyl group of Arg96 and the hydroxyl group of Tyr272. The O6 atom of calyculin A forms a salt bridge with the side chain of Arg221. As a result, the phosphate group of calyculin A is firmly held by two salt bridges and six hydrogen bonds.

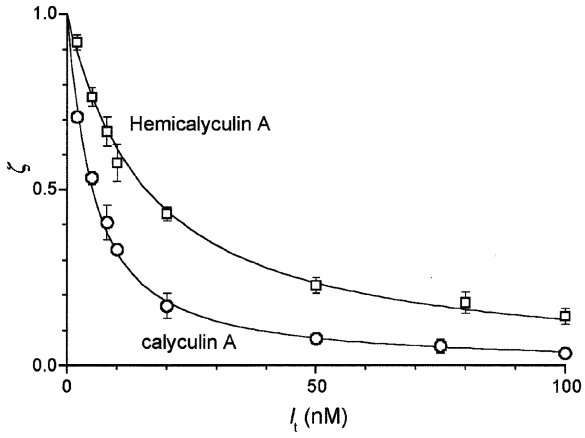

Figure 6. Inhibitory Effects of Calyculin A and Hemicalyculin A of PP1γ

The activity of PP1γ (the total molar concentration, E_t = 2.0 nM) was spectrophotometrically measured using *p*NPP (2 mM) as the substrate. The ratios (ζ) of the steady-state activities in the presence of calyculin A (circles) or hemicalyculin A (boxes) to the activity in their absence are plotted against the total concentration of the inhibitors I_t (see Equation 1). Each symbol represents the average of at least five values. Vertical bars indicating standard errors of means are shown if they are larger than the symbols. Note that the inhibitory activity is considerably retained in hemicalyculin A, which lacks the C29–C37 side chain. See the text for further details.

Calyculin A Binding Site in the Hydrophobic and Acidic Grooves

As mentioned above, PP1 has three grooves on its molecular surface, that is, the hydrophobic groove, the acidic groove, and the C-terminal groove (Figure 3A). Calyculin A is located in the former two grooves through the bifurcation point of the three grooves. The recognition of calyculin A by the PP1 molecule is performed by both hydrophobic and hydrophilic interactions. The recognition site formed by the grooves consists of Arg96 and Arg221.

Hydrophobic interactions were observed between the hydrophobic tail of calyculin A (N1–C10) and the hydrophobic groove of PP1. A similar interaction was observed in the PP1α-MCLR structure. Figure 5B shows the residues located within 3.5 Å of calyculin A, except for the metal ligand residues. The C49 and C50 atoms of calyculin A show hydrophobic interactions with Val223. The C10 and C46 atoms of calyculin A have van der Waals contacts with Tyr134, which forms a hydrogen bond with MCLR in the PP1α-MCLR crystal structure.

Hydrophilic interactions are mainly observed in the catalytic site of PP1, the bifurcation point of the three grooves. The phosphate group of calyculin A forms salt bridges with the side chains of the guanidyl groups of Arg96 and Arg221, as proposed for the substrate bound to PP1 [20]. Hydrogen bonds between the phosphate oxygen and the phenol of Tyr272 and between 13-OH of calyculin A and the guanidyl group of Arg221 were observed. 13-OH also forms an intramolecular hydrogen bond with its phosphate oxygen. 11-OH of calyculin A and the main chain carbonyl oxygen atom of Arg221 are also hydrogen bonded.

In the acidic groove, the oxazole group exhibits a weak contact with Asp220. Neither hydrogen bonds nor salt bridges between calyculin A and the enzyme were observed in the acidic groove. The region between C33 and C37 atoms of calyculin A, which is supposed to have large flexibility in the crystal form, could not be located due to unclear electron densities.

The data of the site-directed mutagenesis of PP1 showed that Tyr272 is of specific importance for the binding of calyculin A [10] and that mutants N124D, H248N, R96A, R221S, and D208A exhibit large decreases in sensivity to calyculin A [11]. As described above, Tyr272, Arg96, and Arg221 bind to calyculin A directly (Figures 5A and 5B), and the residues of Asn124 and His248 are the metal ligands and are included in the network at the active site (Figure 5A). Asp208 forms a hydrogen bond with Arg221. It may contribute the stabilization of Arg221. Moreover, the other mutagenesis data reports that the mutant Y134F showed only a slight difference of IC50 [16]. The fact that no hydrogen bond exists between Tyr134 and calyculin A is consistent with this mutagenesis result.

Inhibitory Effects of Calyculin A and Hemicalyculin A on the *p*-Nitrophenol Phosphate (*p*NPP) Phosphatase Activity of PP1γ

Figure 6 shows the inhibitory effects of calyculin A and hemicalyculin A on the phosphatase activity of PP1γ measured using *p*-nitrophenyl phosphate (*p*NPP; 2 mM) as the substrate. The specific activity of the preparation of PP1γ was 4.25 ± 0.05 μmol P_i liberated/min/mg of protein (total number of measurements, n = 195), which was within the range of the value reported in our previous paper [19]. Calyculin A strongly inhibited this activity in a dose-dependent manner (Figure 6). From the dose-inhibition relationship, the K_i associated with the binding of PP1γ to calyculin A is estimated at 4.1 ± 1 nM (n =

123), which corresponds to a standard free-energy change (ΔG) of -48 kJ mol^{-1}. This K_i value is slightly but significantly larger than the value (1.1 nM) obtained by our previous experiments for the interaction of calyculin A and a native catalytic subunit of PP1 (PP1c) under the same experimental conditions. Alessi et al. [23] reported that the recombinant PP1 isozymes, including PP1γ, were considerably less sensitive to okadaic acid and MCLR than PP1c. As they discussed, the altered sensitivity presumably reflects conformational differences between the expressed isozymes and native PP1c.

The *p*NPP phosphatase activity of PP1γ was also strongly inhibited by hemicalyculin A [8], which lacks the C29–C37 component (Figures 1 and 6). The dose-inhibition data gave a K_i value of 14.8 ± 0.5 nM ($n = 62$), which translates to a ΔG of -45 kJ mol^{-1}. The difference between the $|\Delta G|$ for calyculin A and that for hemicalyculin A is thus only 3 kJ mol^{-1}. Considering the relatively large size of the C29–C37 component, which constitutes about 30% of the total molecular mass of calyculin A, the reduction of the affinity to PP1γ caused by its removal is surprisingly small. It is known that even slight modifications of the rest of the molecule tend to cause a much more drastic reduction of the affinity [8]. The C29–C37 component of calyculin A thus appears to make only a limited contribution to the toxin binding to PP1γ. The invisibility of the terminal amino acid portion in the X-ray crystallography is indicative that this portion is exposed to the solvent and has little or no interaction with the enzyme.

Mechanism of PP1 Inhibition

The revised SAR study of calyculins has disclosed structural units important for the inhibition of PP1. Specifically, the loss of the phosphate group and the modification of 13-OH abolished the inhibitory activity. While isomerization of one or two double bonds in the hydrophobic tail diminished the activity to some extent, the loss of the hydrophobic tail abrogated the activity. The crystal structure of the complex clearly showed the importance of the salt bridges between the phosphate in calyculin A and the two arginine residues in the substrate recognition site. Similarly, the hydrophobic interactions were required to sustain the binding. However, these interactions are not sufficient to explain the reason why the phosphate group in calyculin A is resistant to hydrolysis by the enzyme.

The catalytic mechanism proposed on the basis of the structure of PP1 bound to tungstate dictates that O1 and O3 of the phosphate in the substrate form salt bridges with Arg96 and Arg221, respectively, and O1 and O2 are bonded to the two metal ions so that the hydroxide anion between the metals can attack the phosphorus atom [20]. In the complex of calyculin A and PP1, in spite of the presence of the corresponding salt bridges of two phosphate oxygens with Arg96 and Arg221, the atoms corresponding to O1 and O2 are maintained in the position too far to be accessed by the metals. It is likely that the remaining interaction(s) between calyculin A and PP1 should keep the phosphate group from approaching the metal ions. The hydrogen-donating property of the 11-OH is dispensable because calyculin J, with an ether oxygen on C11, retains the activity [8, 24]. Therefore, it is concluded that the hydrogen bond between 13-OH and Arg221 functions to keep the phosphate group of calyculin A in a position distant enough from the catalytic center. This assumption is in accordance with the total loss of activity in the derivatives modified at 13-OH [8].

Most of known protein phosphatase inhibitors exhibit considerably higher affinity to PP2A than to PP1. With okadaic acid, for example, the ratio of the K_i value for PP1 to that for PP2A (PP1/PP2A ratio) is about 5000 [19, 48, 49]. Although calyculin A also exhibits slightly higher affinity for PP2A than it does for PP1, the difference in the affinities is much smaller with this toxin, which gives a PP1/PP2A ratio of less than 10 [19]. The PP1/PP2A ratio corresponds to a difference in free-energy change of less than 3 kJ/mol. A difference of this magnitude could be attributable to (for example) a very small difference in the relative position of the donor and acceptor of a hydrogen bond. It is, unfortunately, impossible to resolve such a small difference from the present data. Further experiments are necessary to elucidate the structural background for the widely different affinities of the protein phosphatase inhibitors to PP1 and PP2A.

Biological Implications

The catalytic subunits of serine/threonine phosphatases 1 and 2A are subjected to inhibition by various toxins, the so-called okadaic acid class of compounds [25], including cyclic peptides based on compounds such as MCLR [5], the polyketides, including okadaic acid [3] and calyculin A [4], and terpenoids, including cantharidin [6]. It has been shown that the okadaic acid class of natural product inhibitors affects cellular reactions that are controlled by phosphorylation/dephosphorylation mechanisms and may promote tumor formation in some cases [2, 4, 26–33].

In the present study, we reported the first three-dimensional structure of the calyculin A accommodated in the catalytic subunit of serine/threonine phosphatase γ (PP1γ). Numerous investigations of the binding model of natural toxic inhibitors in PP1 have been carried out based on the X-ray crystal structure of rabbit PP1α complexed with MCLR (PP1α-MCLR), as well as those of human PP1γ and those of its complex with tungstate. Therefore, the present structure of PP1γ-calyculin A complex provides direct evidence for understanding the general mechanism of the PP1 inhibition. PP1γ has two metal ions, which are located at the bifurcation point of the Y-shaped grooves on the PP1γ molecular surface. The phosphate group of calyculin A is also located at the bifurcation point, and there are hydrophilic interactions between PP1γ and calyculin A. It therefore can be assumed that the dephosphorylation reaction probably occurs at this point. Between PP1γ and calyclulin A, there are hydrophilic interactions at the bifurcation point as well as hydrophobic interactions at the hydrophobic groove. However, few interactions are observed at the acidic groove. The C-terminal groove of PP1γ in PP1γ-

calyculin A complex is closed. The structures of PP1γ-calyculin A complex, PP1α-MCLR, and PP1γ-okadaic acid complex indicate that the hydrophobic groove plays a dominant role in binding the inhibitors and that the acidic groove does play an additional role. The structure of PP1 in complex with a phosphorylated protein will provide information about how the C-terminal groove functions in molecular recognition.

Experimental Procedures

Preparation and Purification of Protein Phosphatases

A full-length cDNA encoding the γ isoform of PP1 (PP1γ) was expressed in *Escherichia coli* (provided by Dr. Patricia Cohen, Dundee, UK), as described [23]. The expressed PP1γ was purified by sequential chromatography at 4°C on five columns: HiPrep Q-XL, HiPrep SP-XL, phenyl-Sepharose, Sephacryl S-200, and Mono-Q (all purchased from Amersham-Pharmacia Biotech, Uppsala, Sweden). Buffers used for the expression and purification of PP1γ contained 1 mM $MnCl_2$. The purified sample of PP1γ gave a single polypeptide spot at pH 6.0 and an apparent molecular mass of 37 kDa when subjected to two-dimensional electrophoresis (i.e., isoelectric focusing on an IPG gel [Amersham-Pharmacia] in the presence of 8 M urea and 20 mM DTT under a linear gradient of pH 3–10 in 10 cm, which was followed by SDS/PAGE). The molar concentration of PP1γ was determined by a titration procedure [34] using MCLR (provided by Dr. K. Harada, Meijo University, Nagoya, Japan) as the standard.

Crystallization

Purified protein solutions were dialyzed against 10 mM Tris-HCl (pH 7.8) containing 0.3 M NaCl, 0.2 mM $MnCl_2$, and 3 mM dithiothreitol. After dialysis of the protein solution, calyculin A was dissolved in dimethyl sulfoxiside (DMSO), mixed into a protein solution in the 3-fold excess with PP1γ, and incubated on ice for 1 hr. The sitting drop vapor diffusion method was employed for the crystallization. The PP1γ-calyculin A solutions were concentrated to 7.4 mg/ml by using a microconcentrator (Centricon 30; Amicon). Droplets (2 μl) of the protein solution contained 7.4 mg/ml PP1γ-calyculin A, 10 mM Tris-HCl (pH 7.8), 0.3 M NaCl, 0.2 mM $MnCl_2$, and 3 mM dithiothreitol, whereas the reservoir solutions contained 10 mM Tris-HCl (pH 7.8), 20% PEG 3350, and 0.2 M potassium sulfate. Mixtures of protein solution and the same volume of the reservoir solution were equilibrated against the reservoir solution. All crystallizations were carried out at 20°C. The crystals grew to an average size of 0.3 × 0.3 × 0.2 mm. The crystals belong to the space group of $P2_12_12$ with unit cell dimensions of $a = 98.1$ Å, $b = 136.4$ Å, and $c = 61.6$ Å. The asymmetric unit contains two PP1γ-calyculin A complexes.

Data Collection

Intensity data of the PP1γ-calyculin A complex crystals were all collected at room temperature using synchrotron radiation with a MARCCD detector on a beamline station of BL44B2 at SPring-8 (Harima, Japan) and with an ADSC Quantum 4R CCD camera on a beamline of BL6A of the Photon Factory (KEK; Tsukuba, Japan). X-ray diffraction spots of PP1γ-calyculin A complex crystals up to 2.0 Å were collected at SPring-8 (BL44B2). The intensity data were processed by using the programs of HKL2000 [35] package and TRUNCATE [36] (Table 1). Intensity data at 50.0–2.0 Å resolution were obtained with an overall R_{merge} of 7.8% and a completeness of 99.9%.

Phasing and Model Building

The molecular replacement method was applied for the phase determination with the program AMORE [37] in the CCP4 package [36]. The atomic coordinates of the PP1α-MCLR complex (PP1α-MCLR; PDB code 1FJM) were used as a search model. Two clear peaks appeared in the molecular replacement procedures using the reflections between 15.0 and 4.0 Å resolution. The structural model was built by manual fitting to the electron density map by using the program TURBO-FRODO [38]. All structural refinements including the bulk solvent corrections were carried out using the program X-PLOR [39]. The topology and parameter files for calyculin A were generated by the program XPLO2D [40]. Two metal atoms were not included in the refinement procedure to reduce the model bias in the phases and were then added to the model in the last step to the center of the 20 σ peak in the Mn-omitted $F_o - F_c$ electron density map. The superimpositions of the molecules were performed by using the program LSQMAN [41]. The final model was analyzed using the program PROCHECK [42]. The charge distribution of the molecular surface was calculated and represented by using the program GRASP [43]. The molecular models in the figures were drawn by using the programs of MOLSCRIPT [44] and RASTER3D [45].

Dose-Inhibition Analysis

The activity of the PP1γ was measured at 25°C using *p*-nitrophenyl phosphate (*p*NPP) as the substrate, essentially by the method described previously [34]. This artificial substrate is particularly useful for the present purpose because PP1γ shows a considerably high activity against it, which can be very easily and accurately measured by monitoring the elevation of absorbance at 405 nm as a result of liberation of the product *p*-nitrophenol. We have shown that the *p*NPP phosphatase activity of PP1γ exhibits essentially the same susceptibilities to several phosphatase inhibitors (such as okadaic acid, microcystins, and tautomycin) and their derivatives as do its activities toward phosphorylated proteins [46, 47]. The buffer used for the assays contained the following: Tris-base, 40 mM; $MgCl_2$, 34 mM; EDTA (free acid), 4 mM; and DL-dithiothreitol, 4 mM (pH 8.4). No bivalent cation other than Mg^{2+} was added.

In previous experiments on the inhibition of protein phosphatases by their tight binding inhibitors [19, 34, 48, 49], we have shown that the steady-state dose-inhibition relationship at a fixed total enzyme concentration, E_t, is well described by a general model function:

$$\zeta = \zeta\,(I_t) = \frac{E_t - I_t - K_i + \sqrt{(E_t - I_t - K_i)^2 + 4E_tK_i}}{2E_t} \qquad (1)$$

where K_i is the dissociation constant, and $\zeta(I_t)$ denotes the fractional activity at a given total inhibitor concentration, I_t. In the present experiments the K_i values were estimated with the standard errors by fitting this nonlinear model function to the data obtained by dose-inhibition experiments.

Acknowledgments

We would like to thank Drs. S. Adachi and S.-Y. Park of SPring-8 (BL44B2), Harima, Japan, for their kind help in intensity data collection. Thanks are also due to Drs. N. Sakabe, M. Suzuki, and N. Igarashi at the Photon Factory (BL6A and 18B) for their kind help in the X-ray diffraction works, which were performed under the approval of the Photon Factory Advisory Committee (proposal number 2001G159). K.M. is a member of the Structural Biology Sakabe Project, University of Tsukuba. This work was partly supported by grants from the "Research for the Future" Programs of the Japan Society for the Promotion of Science to K.M. (97L00501), S.M. (96I00301), and M.I. (96L00504) and by a Grant-in-Aid for Scientific Reseach (13470365) and a Grant-in-Aid for Exploratory Research (13877287) to A.T.

Received: September 11, 2001
Revised: February 14, 2002
Accepted: March 1, 2002

References

1. Cohen, P. (1989). The structure and regulation of protein phosphatases. Annu. Rev. Biochem. *58*, 453–508.
2. Shenolikar, S., and Nairn, A.C. (1991). Protein phosphatases: recent progress. Adv. Second Messenger Phosphoprotein Res. *23*, 1–121.
3. Takai, A., Bialojan, C., Troschka, M., and Ruegg, J.C. (1987). Smooth muscle myosin phosphatase inhibition and force enhancement by black sponge toxin. FEBS Lett. *217*, 81–84.
4. Ishihara, H., Martin, B.L., Brautigan, D.L., Karaki, H., Ozaki, H., Kato, Y., Fusetani, N., Watabe, S., Hashimoto, K., Uemura, D., et al. (1989). Calyculin A and okadaic acid: inhibitors of protein

phosphatase activity. Biochem. Biophys. Res. Commun. *159*, 871–877.

5. MacKintosh, C., Beattie, K.A., Klumpp, S., Cohen, P., and Codd, G.A. (1990). Cyanobacterial microcystin-LR is a potent and specific inhibitor of protein phosphatases 1 and 2A from both mammals and higher plants. FEBS Lett. *264*, 187–192.
6. Li, Y.M., and Casida, J.E. (1992). Cantharidin-binding protein: identification as protein phosphatase 2A. Proc. Natl. Acad. Sci. USA *89*, 11867–11870.
7. Kato, Y., Fusetani, N., Matsunaga, S., and Hashimoto, K. (1988). Calyculins, potent antitumour metabolites from the marine sponge Discodermia calyx: biological activities. Drugs Exp. Clin. Res. *14*, 723–728.
8. Wakimoto, T., Matsunaga, S., Takai, A., and Fusetani, N. (2002). Insight into binding of calyculin A to protein phosphatase 1. Isolation of hemicalyculin A and chemical transformation of calyculin A. Chem. Biol. *9*, 309–319.
9. Zhang, Z., Zhao, S., Long, F., Zhang, L., Bai, G., Shima, H., Nagao, M., and Lee, E.Y. (1994). A mutant of protein phosphatase-1 that exhibits altered toxin sensitivity. J. Biol. Chem. *269*, 16997–17000.
10. Zhang, L., Zhang, Z., Long, F., and Lee, E.Y. (1996). Tyrosine-272 is involved in the inhibition of protein phosphatase-1 by multiple toxins. Biochemistry *35*, 1606–1611.
11. Huang, H.B., Horiuchi, A., Goldberg, J., Greengard, P., and Nairn, A.C. (1997). Site-directed mutagenesis of amino acid residues of protein phosphatase 1 involved in catalysis and inhibitor binding. Proc. Natl. Acad. Sci. USA *94*, 3530–3535.
12. Goldberg, J., Huang, H.B., Kwon, Y.G., Greengard, P., Nairn, A.C., and Kuriyan, J. (1995). Three-dimensional structure of the catalytic subunit of protein serine/threonine phosphatase-1. Nature *376*, 745–753.
13. Bagu, J.R., Sykes, B.D., Craig, M.M., and Holmes, C.F. (1997). A molecular basis for different interactions of marine toxins with protein phosphatase-1. Molecular models for bound motuporin, microcystins, okadaic acid, and calyculin A. J. Biol. Chem. *272*, 5087–5097.
14. Gauss, C.M., Sheppeck, J.E., 2nd, Nairn, A.C., and Chamberlin, R. (1997). A molecular modeling analysis of the binding interactions between the okadaic acid class of natural product inhibitors and the Ser-Thr phosphatases, PP1 and PP2A. Bioorg. Med. Chem. *5*, 1751–1773.
15. Volter, K.E., Pierens, G.K., Quinn, R.J., Wakimoto, T., Matsunaga, S., and Fusetani, N. (1999). The solution structures of calyculin A and dephosphonocalyculin A by NMR. Bioorg. Med. Chem. Lett. *9*, 717–722.
16. McCready, T.L., Islam, B.F., Schmitz, F.J., Luu, H.A., Dawson, J.F., and Holmes, C.F. (2000). Inhibition of protein phosphatase-1 by clavosines A and B. Novel members of the calyculin family of toxins. J. Biol. Chem. *275*, 4192–4198.
17. Volter, K.E., Embrey, K.J., Pierens, G.K., and Quinn, R.J. (2001). A study of the binding requirements of calyculin A and dephosphonocalyculin A with PP1, development of a molecular recognition model for the binding interactions of the okadaic acid class of compounds with PP1. Eur. J. Pharm. Sci. *12*, 181–194.
18. Kato, Y., Fusetani, N., Matsunaga, S., Hashimoto, K., Fujita, S., and Furuya, T. (1986). Calyculin A, a novel antitumor metabolite from the marine sponge *Discodermia calyx*. J. Am. Chem. Soc. *108*, 2780–2781.
19. Takai, A., Sasaki, K., Nagai, H., Mieskes, G., Isobe, M., Isono, K., and Yasumoto, T. (1995). Inhibition of specific binding of okadaic acid to protein phosphatase 2A by microcystin-LR, calyculin-A and tautomycin: method of analysis of interactions of tight-binding ligands with target protein. Biochem. J. *306*, 657–665.
20. Egloff, M.-P., Cohen, P.T.W., Reinemer, P., and Barford, D. (1995). Crystal structure of the catalytic subunit of human protein phosphatase 1 and its complex with tungstate. J. Mol. Biol. *254*, 942–959.
21. Maynes, J.T., Bateman, K.S., Cherney, M.M., Das, A.K., Luu, H.A., Holmes, C.F., and James, M.N. (2001). Crystal structure of the tumor-promoter okadaic acid bound to protein phosphatase-1. J. Biol. Chem. *276*, 44078–44082.
22. Connor, J.H., Kleeman, T., Barik, S., Honkanen, R.E., and Shenolikar, S. (1999). Importance of the β12-β13 loop in protein phosphatase-1 catalytic subunit for inhibition by toxins and mammalian protein inhibitors. J. Biol. Chem. *274*, 22366–22372.
23. Alessi, D.R., Street, A.J., Cohen, P., and Cohen, P.T. (1993). Inhibitor-2 functions like a chaperone to fold three expressed isoforms of mammalian protein phosphatase-1 into a conformation with the specificity and regulatory properties of the native enzyme. Eur. J. Biochem. *213*, 1055–1066.
24. Matsunaga, S., Wakimoto, T., and Fusetani, N. (1997). Isolation of four new calyculins from the marine sponge *Discodermia calyx*. J. Org. Chem. *62*, 2640–2642.
25. Fujiki, H., Suganuma, M., Nishiwaki, S., Yoshizawa, S., Yatsunami, J., Matsushima, R., Furuya, H., Okabe, S., Matsunaga, S., and Sugimura, T. (1992). Specific mechanistic aspects of animal tumor promoters: the okadaic acid pathway. Prog. Clin. Biol. Res. *374*, 337–350.
26. Bialojan, C., and Takai, A. (1988). Inhibitory effect of a marine-sponge toxin, okadaic acid, on protein phosphatases. Specificity and kinetics. Biochem. J. *256*, 283–290.
27. Hescheler, J., Mieskes, G., Ruegg, J.C., Takai, A., and Trautwein, W. (1988). Effects of a protein phosphatase inhibitor, okadaic acid, on membrane currents of isolated guinea-pig cardiac myocytes. Pflugers Arch. *412*, 248–252.
28. Honkanen, R.E., Zwiller, J., Moore, R.E., Daily, S.L., Khatra, B.S., Dukelow, M., and Boynton, A.L. (1990). Characterization of microcystin-LR, a potent inhibitor of type 1 and type 2A protein phosphatases. J. Biol. Chem. *265*, 19401–19404.
29. Sassa, T., Richter, W.W., Uda, N., Suganuma, M., Suguri, H., Yoshizawa, S., Hirota, M., and Fujiki, H. (1989). Apparent "activation" of protein kinases by okadaic acid class tumor promoters. Biochem. Biophys. Res. Commun. *159*, 939–944.
30. Suganuma, M., Fujiki, H., Suguri, H., Yoshizawa, S., Hirota, M., Nakayasu, M., Ojika, M., Wakamatsu, K., Yamada, K., and Sugimura, T. (1988). Okadaic acid: an additional non-phorbol-12-tetradecanoate-13-acetate-type tumor promoter. Proc. Natl. Acad. Sci. USA *85*, 1768–1771.
31. Suganuma, M., Suttajit, M., Suguri, H., Ojika, M., Yamada, K., and Fujiki, H. (1989). Specific binding of okadaic acid, a new tumor promoter in mouse skin. FEBS Lett. *250*, 615–618.
32. Suganuma, M., Fujiki, H., Furuya-Suguri, H., Yoshizawa, S., Yasumoto, S., Kato, Y., Fusetani, N., and Sugimura, T. (1990). Calyculin A, an inhibitor of protein phosphatases, a potent tumor promoter on CD-1 mouse skin. Cancer Res. *50*, 3521–3525.
33. Yoshizawa, S., Matsushima, R., Watanabe, M.F., Harada, K., Ichihara, A., Carmichael, W.W., and Fujiki, H. (1990). Inhibition of protein phosphatases by microcystins and nodularin associated with hepatotoxicity. J. Cancer Res. Clin. Oncol. *116*, 609–614.
34. Takai, A., and Mieskes, G. (1991). Inhibitory effect of okadaic acid on the p-nitrophenyl phosphate phosphatase activity of protein phosphatases. Biochem. J. *275*, 233–239.
35. Otwinoski, Z., and Minor, W. (1997). Processing of X-ray diffraction data collected in oscillation mode. Methods Enzymol. *276*, 307–326.
36. Collaborative Computational Project 4. (1994). The CCP4 suite: programs for protein crystallography. Acta Crystallogr. D Biol. Crystallogr. *50*, 760–763.
37. Navaza, J. (1994). AMoRe: atomated package for molecular replacement. Acta Crystallogr. A *50*, 157–163.
38. Roussel, A., and Cambillau, C. (1992). TURBO FRODO Program (Mountain View, CA: Silicon Graphics Geometry Partners Directory).
39. Brunger, A.T. (1992). X-PLOR Version 3.1 Manual. X-PLOR (New Haven, CT: Yale University Press).
40. Kleywegt, G.J., and Jones, T.A. (1997). Model building and refinement practice. Methods Enzymol. *277*, 208–230.
41. Kleywegt, G.J. (1996). Use of non-crystallographic symmetry in protein structure refinement. Acta Crystallogr. D Biol. Crystallogr. *52*, 842–857.
42. Laskowski, R.A., MacArthur, M.W., Moss, D.S., and Thornton, J.M. (1993). PROCHECK: a program to check the stereochemical quality of protein structures. J. Appl. Crystallogr. *26*, 283–291.
43. Nicholls, A., Sharp, K.A., and Honig, B. (1991). Protein folding

and association: insights from the interfacial and thermodynamic properties of hydrocarbons. Proteins *11*, 281–296.
44. Kraulis, P.J. (1991). MOLSCRIPT: a program to produce both detailed and schematic plots of protein structure. J. Appl. Crystallogr. *24*, 946–950.
45. Merritt, E.A., and Murthy, M.E.P. (1994). Raster3D version 2.0—program for photorealistic molecular graphics. Acta Crystallogr. D Biol. Crystallogr. *50*, 869–873.
46. Takai, A., Tsuboi, K., Koyasu, M., and Isobe, M. (2000). Effects of the hydrophobic C-1−C-16 segment of tautomycin on its affinity to type-1 and type-2A protein phosphatases. Biochem. J. *350*, 81–88.
47. Ito, E., Takai, A., Kondo, F., Masui, H., Imanishi, S., and Harada, K. (2001). Comparison of protein phosphatase inhibitory activity and apparent toxicity of microcystins and related compounds. Toxicon, in press.
48. Takai, A., Murata, M., Torigoe, K., Isobe, M., Mieskes, G., and Yasumoto, T. (1992). Inhibitory effect of okadaic acid derivatives on protein phosphatases. A study on structure-affinity relationship. Biochem. J. *284*, 539–544.
49. Takai, A., Ohno, Y., Yasumoto, T., and Mieskes, G. (1992). Estimation of the rate constants associated with the inhibitory effect of okadaic acid on type 2A protein phosphatase by time-course analysis. Biochem. J. *287*, 101–106.

Accession Numbers

The atomic coordinates have been deposited in the Protein Data Bank under accession code 1IT6.